Structure of finite two-dimensional Yukawa lattices: Dust crystals

Hiroo Totsuji,* Chieko Totsuji, and Kenji Tsuruta
Department of Electrical and Electronic Engineering, Okayama University, Tsushimanaka 3-1-1, Okayama 700-8530, Japan
(Received 6 November 2000; revised manuscript received 2 July 2001; published 12 November 2001)

Dust particles in plasmas are often confined near the boundary between the plasma bulk and the sheath where the gravitation is balanced by electrostatic force. To keep dust particles from running away horizontally, an electrostatic potential is usually applied to the electrode surrounding these dusty plasmas and, under appropriate conditions, we have finite two-dimensional lattices of dust particles. Modeling the interaction between dust particles as the isotropic Yukawa interaction, structures of finite two-dimensional Yukawa systems at low temperatures have been analyzed both by numerical simulations and variational methods. The effect of the correlation energy between dust particles is shown to play an important role in the formation of the one-body distribution in these systems.

DOI: 10.1103/PhysRevE.64.066402 PACS number(s): 52.65.Yy, 52.27.Lw, 52.27.Jt

I. INTRODUCTION

Dusty plasmas have provided us with a unique system where the role of the Coulomb interaction in its static and dynamic properties can be clearly observed experimentally. One of typical phenomena is the formation of macroscopic plasma crystals, observed by the charge-coupled device camera or even by naked eyes, where obviously the strong Coulomb coupling between dust particles is the essential agent for such structures [1–4]. We have shown that the correlation energy between dust particles plays an important role in determining the structure of finite Coulomb crystals [5–7]. In this paper, we present another example indicating the importance of the Coulomb interaction in the structure of dusty plasma crystals through the result of a numerical simulation and theoretical analysis.

Dust particles in plasmas usually appear near the horizontal boundary between the plasma bulk and the sheath where the gravitational force is balanced by the levitation of the static electric field in the sheath, and they are vertically trapped. Under appropriate conditions, dust particles are also confined horizontally and one can have finite quasi-two-dimensional dusty plasma crystals [8,9].

Regarding dusty plasmas as a system of Yukawa particles confined in a vertical trap, we have shown that its structure changes discretely as a result of the competition between vertical confinement (around the equilibrium position) and mutual repulsion [5–7]. The strength of vertical confinement is determined by the charge density in the sheath and, when it is strong enough, we may realize a two-dimensional system of dust particles in a horizontal plane [5]. In experiments, negatively biased electrodes are usually placed in order to keep dust particles from running away horizontally. We thus have a planar system of dust particles, which is confined also in the lateral directions by the potential of electrodes.

The behavior of finite two-dimensional crystals has attracted much interest as an object of statistical physics and dusty plasma crystals have been analyzed from such viewpoint [10–12]. The effect of the Coulomb interaction in their static structures, however, does not seem to have been fully discussed. In what follows, we analyze the structure of two-dimensional dust crystals taking the correlation energy between dust particles into account [13].

II. POTENTIAL STRUCTURE

We take the z axis in the direction opposite to the gravitation and express the coordinates as $\mathbf{r}=(\mathbf{R},z)$. We adopt the ion matrix sheath model [14] with the sheath in the domain $z<0$. We assume that the density of charges in the sheath (not including those of dust particles) is nearly constant at least in the domain where dust crystals are formed and denote the density by en_{sh}, e being the elementary charge. In the domain $z<0$, the combination of the gravitational potential mgz and the electrostatic potential $2\pi qen_{sh}z^2$ forms a potential well for a dust particle of mass m and charge $-q$ <0 [7]

$$\phi_{ext}^{(1)}(z<0)=mgz+2\pi qen_{sh}z^2=\phi_{ext}(z_0)+\frac{k}{2}(z-z_0)^2, \tag{2.1}$$

where

$$k=4\pi qen_{sh} \tag{2.2}$$

and

$$z_0=-\frac{mg}{4\pi qen_{sh}}=-\frac{g}{4\pi en_{sh}}\frac{m}{q}<0. \tag{2.3}$$

Under only the one-dimensional confinement in the z direction described above, dust particles will expand horizontally and we cannot maintain their surface density: The reduction of the surface density lowers the total energy of the system. In real experiments, such an expansion is limited by some mechanism coming from either the intentionally placed limiting electrode or the size of the experimental apparatus. In numerical simulations, the surface density is forced to remain constant usually by the periodic boundary conditions [5–7]. Our previous analyses of dusty plasmas in the one-

*Email address: totsuji@elec.okayama-u.ac.jp

dimensional confinement have implicitly focused on their behavior in the central part of the system in real experiments, where the system can be regarded as uniform in horizontal directions [5–7].

Let us assume that we place a uniformly charged ring electrode of radius R_0 in the plane $z=z_0$. Then its charge density may be given by

$$\rho_{ring}(\mathbf{r})=\frac{Q}{2\pi R_0}\delta(R-R_0)\,\delta(z-z_0), \tag{2.4}$$

where Q is the total charge on the electrode. The Coulomb potential due to this ring electrode is calculated as

$$\phi_{ring}(\mathbf{r})=\frac{Q}{(2RR_0)^{1/2}t}F\left(\frac{1}{4},\frac{3}{4},1;t^{-2}\right). \tag{2.5}$$

Here $F(\alpha,\beta,\gamma;x)$ is the Gauss's hypergeometric function and $t=[R_0^2+R^2+(z-z_0)^2]/2RR_0$. When $R^2+(z-z_0)^2 \ll R_0^2$, $\phi_{ring}(\mathbf{r})$ is approximately given by

$$\phi_{ring}(\mathbf{r})\sim\frac{Q}{R_0}\left[1+\frac{1}{4}\frac{R^2-2(z-z_0)^2}{R_0^2}\right]. \tag{2.6}$$

When we take the effect of screening into account, Eq. (2.5) becomes

$$\phi_{ring}(\mathbf{r})=\int d\mathbf{r}'\frac{\exp(-|\mathbf{r}-\mathbf{r}'|/\lambda)}{|\mathbf{r}-\mathbf{r}'|}\rho_{ring}(\mathbf{r}'). \tag{2.7}$$

Here λ is the screening length. When $R^2+(z-z_0)^2 \ll R_0^2$, we have

$$\phi_{ring}(\mathbf{r})\sim\frac{Q}{R_0}\exp(-R_0/\lambda)\left[1+\frac{1}{4}\left(1+\frac{R_0}{\lambda}+\frac{R_0^2}{\lambda^2}\right)\frac{R^2}{R_0^2}-\frac{1}{2}\left(1+\frac{R_0}{\lambda}\right)\frac{(z-z_0)^2}{R_0^2}\right]. \tag{2.8}$$

Since we may express the horizontal limiting mechanism by some electrostatic potential due to external charges $\phi_{ext}^{(2)}$, its effect may be given generally by

$$\phi_{ext}^{(2)}(\mathbf{r})\sim\phi_{ext}^{(2)}(0,z_0)+\frac{K}{2}R^2-K'(z-z_0)^2. \tag{2.9}$$

The potential of the external charges $\phi_{ext}^{(2)}$ alone does not have the minimum around $(\mathbf{R},z)=(0,z_0)$: When $\lambda=\infty$, $K=K'$ and $\Delta\phi_{ext}^{(2)}(\mathbf{r})=0$. Combined with the potential $\phi_{ext}^{(1)}(z<0)$ in the sheath, however, we have a potential structure

$$\phi_{ext}(\mathbf{r})=\phi_{ext}^{(1)}(\mathbf{r})+\phi_{ext}^{(2)}(\mathbf{r})\sim\phi_{ext}(0,z_0)+\frac{K}{2}R^2+\frac{k'}{2}(z-z_0)^2, \tag{2.10}$$

where dust particles are confined both vertically and horizontally, if

$$k'=k-2K'>0. \tag{2.11}$$

III. PARAMETERS

We assume that the interaction between dust particles is given by the repulsive Yukawa interaction

$$\frac{q^2}{r}\exp\left(-\frac{r}{\lambda}\right). \tag{3.1}$$

In what follows, we mainly consider the case where dust particles are on a horizontal plane and we may neglect the effect of the ion flow in interactions between particles. The formation of ion clouds below dust particles may lead to additional dipole nature of interactions. Their effect on horizontal structures, however, is much smaller than the one on vertical structures, such as, alignment of dust particles.

At low temperatures, the structure of this dusty plasma confined by the potential $\phi_{ext}(\mathbf{r})$ is determined by the parameters k', K, and the total number of particles. In this paper, we assume that

$$k'\sim k\gg K>0, \tag{3.2}$$

and the system takes a form of thin pancake. The vertical thickness is determined by the competition between the vertical confinement and the mutual repulsion [5,7]. Since the mutual distance of dust particles may be represented by the surface density N_S as $a=1/(\pi N_S)^{1/2}$, such a competition is characterized by the parameter η defined, as in our previous analyses [5,7], by

$$\eta=\frac{\pi^{1/2}}{2}\frac{ka^2/2}{q^2/a}\sim\left(\frac{e}{q}\right)\left(\frac{n_{sh}}{N_S^{3/2}}\right). \tag{3.3}$$

We have shown that the system undergoes structural transitions according to the value of η and, when η is sufficiently large, the system reduces to a single layer [5].

In the following, we consider the case where the dusty plasma collapses into a single layer and shift the z axis so that $z_0=0$. The total potential energy in our system composed of N particles

$$\sum_{i>j}^{N}\frac{q^2}{R_{ij}}\exp\left(-\frac{R_{ij}}{\lambda}\right)+\frac{1}{2}K\sum_{i}^{N}R_i^2 \tag{3.4}$$

is rewritten into the form

$$\frac{q^2}{\lambda}\left[\sum_{i>j}^{N}\frac{1}{R'_{ij}}\exp(-R'_{ij})+\frac{1}{2\alpha}\sum_{i}^{N}(R'_i)^2\right], \tag{3.5}$$

where

$$\alpha=\frac{q^2}{K\lambda^3}. \tag{3.6}$$

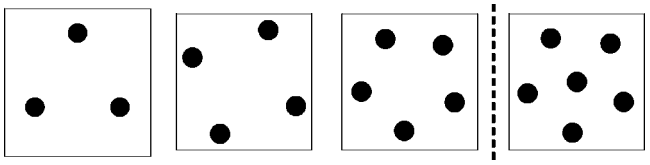

FIG. 1. Structures of the finite two-dimensional Yukawa dusty plasma crystal in the ground state for a small number of particles. System size changes with α while the structure remains the same.

Here quantities with the prime are measured by the screening length λ; $R'_{ij}=R_{ij}/\lambda=|\mathbf{R}_i-\mathbf{R}_j|/\lambda$, and $R'_i=R_i/\lambda$. Equation (3.5) indicates that our system at low temperatures is characterized by the parameters α and the total number of particles N. When α is large, the lateral confinement is weak or the screening is strong; the system is expected to behave as the one with short-ranged interactions. When α is small, the lateral confinement is strong or the screening is weak; the system is expected to behave as finite Coulombic one.

Since the parameter α may seem to lack the direct correspondence to experiments, we here present some numbers based on the results that will be given in Sec. V. The mean distance between particles a is roughly given by

$$\frac{a}{\lambda}=\left(\frac{8\alpha}{N}\right)^{1/4}. \tag{3.7}$$

When $N=10^4$, we have $a/\lambda=1.68$ and $a/\lambda=0.168$ for $\alpha=10^4$ and $\alpha=1$, respectively. These numbers are within the range of parameters of usual dusty plasma experiments.

IV. STRUCTURES AT LOW TEMPERATURES: MOLECULAR DYNAMICS SIMULATION

We have performed molecular dynamics simulations on our confined two-dimensional Yukawa system. The force on each particle and the total potential have been evaluated both by the direct computation and by the fast multipole method (the tree code) [15]. The temperature of the system has been kept constant by the Nosé-Hoover method [16]. Slowly decreasing the temperature, we have obtained the structures at low temperatures.

When the number of particles is small, we have the ring-type configuration or the star configuration according to the number N as shown in Fig. 1. The ground state is given by the ring-type configurations for $N\leqslant 5$ or by the star configuration for $N\geqslant 6$, *irrespective of* the value of the parameter α.

With the increase of the number of particles, the central part of the system is organized into the triangular lattice, while the ring-type configurations remain on the periphery: A regular lattice cannot be extended to the whole system and the existence of lattice defects is inevitable. Some examples are shown in Fig. 2. Since we have many local minima of the total energy, it becomes very difficult to find computationally the global minimum when the number of particles is of the order of or larger than 100.

The density of particles is expressed as $\rho(\mathbf{R})\delta(z)$ and the total number of particles N is related to $\rho(\mathbf{R})$ by

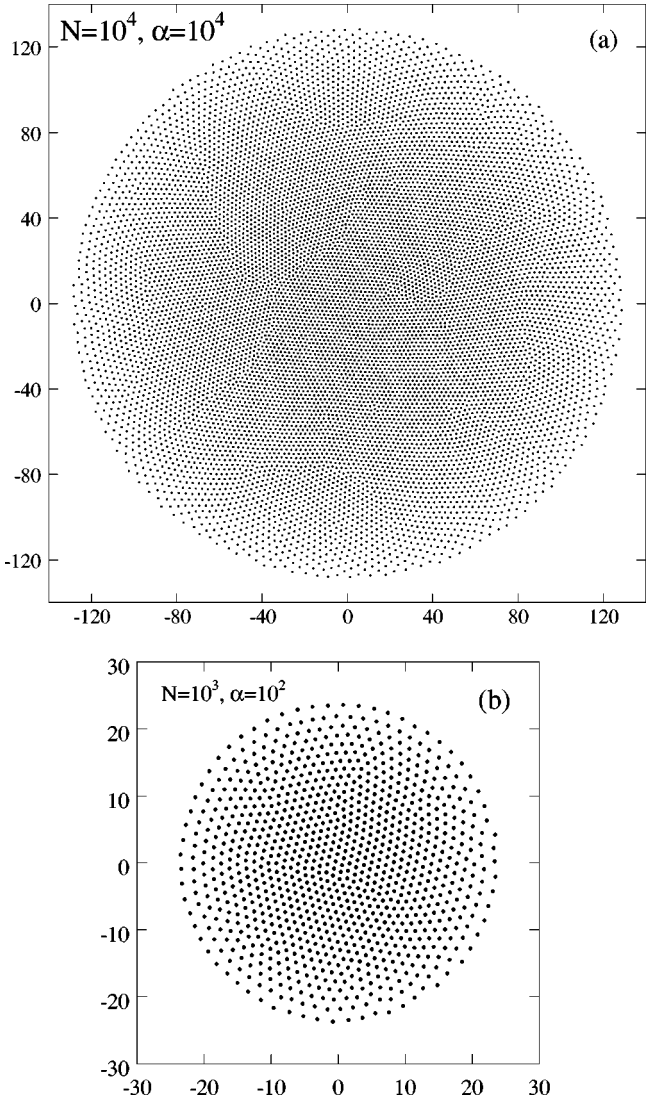

FIG. 2. Examples of structures of the finite two-dimensional Yukawa dusty plasma crystal at low temperatures for a large and intermediate number of particles. Coordinates are normalized by the screening length. (a) $N=10^4$, $\alpha=10^4$ and (b) $N=10^3$, $\alpha=10^2$.

$$\int d\mathbf{R}\rho(\mathbf{R})=N. \tag{4.1}$$

In the case of relatively large number of particles on a plane, we may describe the distribution of particles by the isotropic surface density $\rho(\mathbf{R})=\rho(R)$, which is not so sensitive to the specific local minimum the system is located. Some results are given in Fig. 3. The maximum radius of distribution R_m is shown in Fig. 4.

When fitted to parabolic function of radius, these distribution functions are approximately expressed by a parametrized formula

$$\lambda^2\rho(R)=\frac{c_1}{\alpha^{1/2}}-\frac{c_2}{\alpha}\left(\frac{R}{\lambda}\right)^2, \tag{4.2}$$

where, for example,

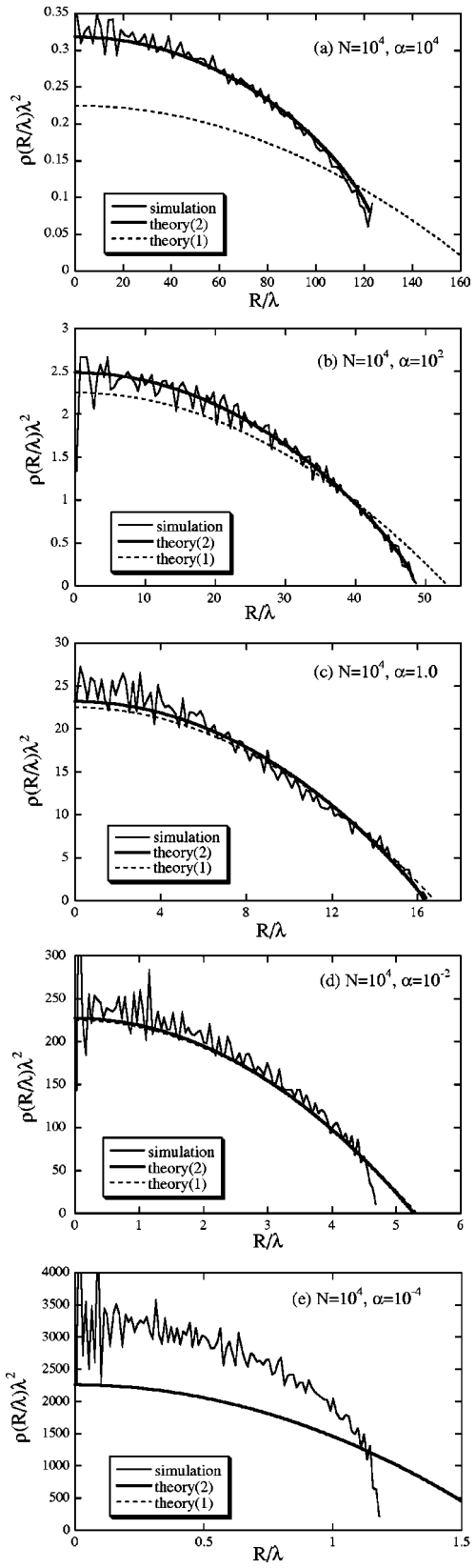

FIG. 3. Radial distribution in finite two-dimensional Yukawa dusty plasma crystals for $N=10^4$. Thick solid lines and broken lines are theoretical results with [theory (2)] and without cohesive energy [theory(1)], respectively. (a) $\alpha=10^4$, (b) 10^2, (c) 1.0, (d) 10^{-2}, and (e) 10^{-4}.

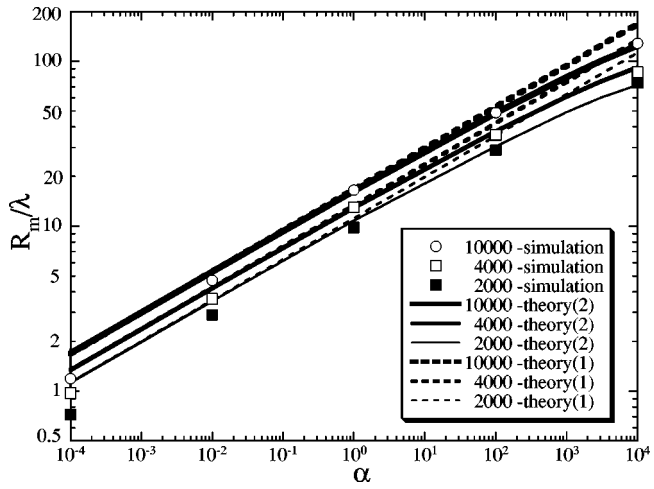

FIG. 4. Radius of the two-dimensional Yukawa dusty plasma crystal for a large number of particles. Symbols are results of simulations. Solid and broken lines are theoretical results with [theory (2)] and without cohesive energy [theory (1)], respectively.

$$c_1 \sim 1.5N^{1/3}, \quad c_2 \sim 0.11, \tag{4.3}$$

for $500 \leqslant N \leqslant 10^4$. Here the power 1/3 is adopted *ad hoc* from the inverse of integers. In the light of the results in Sec. V, one may expect 1/2 instead of 1/3 as the power of N. In that case, we have a formula of the form (4.2) with

$$c_1 \sim 0.35N^{1/2}, \quad c_2 \sim 0.11, \tag{4.4}$$

for $500 \leqslant N \leqslant 10^4$. The fitting with Eq. (4.3) is slightly better than that with Eq. (4.4) for this range of N. The error of this simple interpolation (4.2), however, amounts at most to 20–30 % and is not so sensitive to the power of N. Theoretical results with much better accuracy at least for $\alpha > 1$ will be given in Sec. V.

V. STRUCTURES AT LOW TEMPERATURES: VARIATIONAL ANALYSIS

When the Yukawa particles are distributed uniformly on a plane $z=0$ with the density $\rho(\mathbf{R})\delta(z)=\rho_0\delta(z)$, the potential at $(\mathbf{R},z)$, $\phi(\mathbf{R},z)$, due to these particles is given by

$$\phi(\mathbf{R},z) = \int d\mathbf{r}' \frac{-q}{|\mathbf{r}-\mathbf{r}'|} \exp(-|\mathbf{r}-\mathbf{r}'|/\lambda)\rho(\mathbf{R}')\delta(z')$$
$$= 2\pi(-q)\lambda\rho_0 \exp(-|z|/\lambda). \tag{5.1}$$

Since the interaction energy is written as

$$\frac{1}{2}\int d\mathbf{r}\phi(\mathbf{R},z)(-q)\rho(\mathbf{R})\delta(z) = \int d\mathbf{R}\pi q^2\lambda\rho_0^2, \tag{5.2}$$

the interaction energy per unit area is given by $\pi q^2 \lambda \rho_0^2$.

Let us assume that the distribution of Yukawa particles in our finite system does not depend on the radial distance R and is given by

$$\rho(\mathbf{R}) = \rho_0 \theta(R_m - R), \tag{5.3}$$

where R_m is the radius of distribution and θ is the unit step function. When the edge effect can be neglected, the interaction energy between particles U_{int} may be estimated as

$$U_{int}=\int_{R<R_m} d\mathbf{R}\pi q^2\lambda\rho_0^2=\pi^2 q^2\lambda\rho_0^2 R_m^2. \tag{5.4}$$

The total potential energy of the system is then given by

$$U_{int}+U_{ext}, \tag{5.5}$$

where U_{ext} is the total external potential

$$U_{ext}=\int_{R<R_m} d\mathbf{R}\frac{1}{2}KR^2\rho_0=\frac{1}{4}\pi K\rho_0 R_m^4. \tag{5.6}$$

Minimizing the total potential energy with N kept fixed, we have

$$\rho_0\lambda^2=\frac{N^{1/2}}{2\pi\alpha^{1/2}} \tag{5.7}$$

and

$$R_m=R_0, \tag{5.8}$$

where

$$\left(\frac{R_0}{\lambda}\right)^4=4\alpha N. \tag{5.9}$$

The above results are to be compared with those obtained by simulations shown in Fig. 3. Though the order of magnitude is estimated correctly, it is clear that the assumption of constant density is too simple to reproduce the results of simulations.

Let us now assume that the surface density depends on the radial position as

$$\rho(R)\,\theta(R_m-R) \tag{5.10}$$

and let us adopt the local density approximation. The interaction energy may then be expressed as

$$U_{int}=\int_{R<R_m} d\mathbf{R}\pi q^2\lambda\rho(R)^2. \tag{5.11}$$

The external potential is given by

$$U_{ext}=\int_{R<R_m} d\mathbf{R}\frac{1}{2}KR^2\rho(R). \tag{5.12}$$

Let us find $\rho(R)$ and R_m that minimize the value of $U_{int}+U_{ext}$ under the condition (4.1) (see the Appendix). The variation with respect to $\rho(R)$ leads to

$$\int_{R<R_m} d\mathbf{R}\left[2\pi q^2\lambda\rho(R)+\frac{1}{2}KR^2\right]\delta\rho(R)=0 \tag{5.13}$$

and

$$\int_{R<R_m} d\mathbf{R}\delta\rho(R)=0. \tag{5.14}$$

Denoting the Lagrange's multiplier by μ, we have

$$2\pi q^2\lambda\rho(R)=\mu-\frac{1}{2}KR^2, \tag{5.15}$$

and the value of μ is determined by Eq. (4.1). Taking the variation also with respect to R_m, we have finally

$$\mu=\frac{1}{2}KR_m^2, \tag{5.16}$$

$$\lambda^2\rho(R)=\frac{1}{4\pi\alpha}\left[\left(\frac{R_1}{\lambda}\right)^2-\left(\frac{R}{\lambda}\right)^2\right], \tag{5.17}$$

and the maximum radius $R_m=R_1=2^{1/4}R_0$ or

$$\left(\frac{R_1}{\lambda}\right)^4=2\left(\frac{R_0}{\lambda}\right)^4=8\alpha N. \tag{5.18}$$

The results (5.17) and (5.18) are plotted in Figs. 3 and 4. We observe that, when $\alpha\gg 1$ or $\alpha\ll 1$, they largely underestimate the density and, therefore, overestimate the maximum radius. This indicates that the inclusion of the effect of ordering between particles may be necessary in order to fill the gap between theoretical estimation and simulations: The formation of order reduces the total interaction energy due to negative cohesive (or correlation) energy and, therefore, the system can have larger density or smaller maximum radius.

The cohesive energy of the two-dimensional Yukawa system at low temperatures may be approximately given by that of the two-dimensional Yukawa lattice. The value (per unit area) of the latter with the uniform surface density ρ_0 is expressed by a function $e_{coh}(1/\lambda\rho_0^{1/2})$ as [6]

$$q^2\rho_0^{3/2}e_{coh}\left(\frac{1}{\lambda\rho_0^{1/2}}\right). \tag{5.19}$$

Again within the local density approximation, the total energy is given by

$$\int_{R<R_m} d\mathbf{R}\left[\pi q^2\lambda\rho^2(R)+\frac{1}{2}KR^2\rho(R)+q^2\rho(R)^{3/2}e_{coh}(1/\lambda\rho(R)^{1/2})\right] \tag{5.20}$$

and we denote the maximum radius in this approximation by R_2. The function $e_{coh}(1/\lambda\rho_0^{1/2})$ is approximately given by

$$e_{coh}\left(\frac{1}{\lambda\rho_0^{1/2}}\right)=-a+\frac{b}{\lambda\rho_0^{1/2}}, \tag{5.21}$$

where, for example, in the range of $\rho(R)$ affected most significantly by e_{coh} (see Fig. 3),

$$a/\pi^{1/2}\sim 1.0, \quad b/\pi^{1/2}\sim 0.3\pi^{-1/2}$$

$$\text{for} \quad 0.3\pi^{1/2}<\frac{1}{\lambda\rho_0^{1/2}}<1.7\pi^{1/2}. \tag{5.22}$$

When we take the cohesive energy between particles into account based on the local approximation, we thus have

$$\int_{R<R_m} d\mathbf{R}\left[2\pi q^2\lambda\rho(R)+\frac{1}{2}KR^2 - a\frac{3}{2}q^2\rho(R)^{1/2}+\frac{bq^2}{\lambda}\right]\delta\rho(R) = 0 \tag{5.23}$$

and Eq. (5.14). The density is determined by

$$\lambda^2\rho(R)-\frac{3a}{4\pi}[\lambda^2\rho(R)]^{1/2}=\mu-\frac{b}{2\pi}-\frac{1}{4\pi\alpha}\left(\frac{R}{\lambda}\right)^2 \tag{5.24}$$

and the Lagrange's multiplier μ and the radius $R_m=R_2$ is determined by taking Eq. (4.1) into account (see the Appendix). The final results are

$$\lambda^2\rho(R)=\frac{1}{4\pi\alpha}\left[\left(\frac{R_2}{\lambda}\right)^2-\left(\frac{R}{\lambda}\right)^2\right]+\frac{3a}{4\pi}\left[\frac{1}{4\pi\alpha}\left[\left(\frac{R_2}{\lambda}\right)^2-\left(\frac{R}{\lambda}\right)^2\right]+\left(\frac{a}{8\pi}\right)^2\right]^{1/2}+\frac{5a^2}{32\pi^2}, \tag{5.25}$$

where $R_2(<R_1)$ is determined by

$$8\alpha N=\left(\frac{R_2}{\lambda}\right)^4+\frac{2a}{\pi^{1/2}}\alpha^{1/2}\left\{\left[\left(\frac{R_2}{\lambda}\right)^2+\frac{a^2}{16\pi}\alpha\right]^{3/2}-\left(\frac{a^2}{16\pi}\alpha\right)^{3/2}\right\}+\frac{5a^2}{4\pi}\alpha\left(\frac{R_2}{\lambda}\right)^2. \tag{5.26}$$

The results are plotted in Figs. 3 and 4. We observe that when the parameter α satisfies the condition

$$\alpha>1, \tag{5.27}$$

results of numerical simulations for both the distribution function and the maximum radius are reproduced by the expressions (5.25) and (5.26) to a very good accuracy.

In the case where

$$\alpha\ll 1, \tag{5.28}$$

the maximum radius becomes comparable with or smaller than the screening length. In other words, the range of the potential from a particle in the system λ becomes comparable with or larger than the system radius. The local density approximation may not be applicable in this domain and this may be the main reason for the deviation from the results of numerical experiments.

VI. CONCLUSION

The two-dimensional Yukawa system confined by the (lateral) parabolic potential at low temperatures has been analyzed by numerical simulations and variational calculations. When the number of particles is large, numerical results for the one-body distribution are expressed by a simple interpolation formula. It has been shown that, when the screening length is larger than the radial system size, the one-body distribution at low temperatures obtained by numerical simulations is reproduced by minimizing the total energy of the system within the local density approximation, where the inclusion of the cohesive (correlation) energy is of an essential importance.

ACKNOWLEDGMENTS

The authors thank Ken'ichi Kamon and Tokunari Kishimoto for their numerical work in the early stage of this investigation. This work has been partly supported by the Grants-in-Aid for Scientific Researches of the Ministry of Education, Science, Sports, and Culture of Japan, Grant Nos. 08458109 and 11480110.

APPENDIX

We minimize the integral

$$\int_{R<R_m} d\mathbf{R}G[\rho](R) \tag{A1}$$

under the condition

$$\int_{R<R_m} d\mathbf{R}\rho=N, \tag{A2}$$

where the integrand of $U_{int}+U_{ext}$ is expressed as $G[\rho](R)$. The variation with respect to ρ with fixed R_m gives

$$\frac{\delta G[\rho]}{\delta\rho}=\mu, \tag{A3}$$

where the Lagrange's multiplier μ is determined by Eq. (A2) as $\mu=\mu(R_m)$. Substituting the result into Eq. (A1), we minimize Eq. (A1) further with respect to R_m by taking the variation as

$$2\pi R_m G[\rho](R_m)+\int_{R<R_m} d\mathbf{R}\frac{\delta G[\rho]}{\delta\rho}\frac{\partial\rho}{\partial\mu}\frac{d\mu}{dR_m} = 2\pi R_m G[\rho](R_m)+\mu\int_{R<R_m} d\mathbf{R}\frac{\partial\rho}{\partial\mu}\frac{d\mu}{dR_m}=0. \tag{A4}$$

Since the variation of Eq. (A2) with respect to R_m gives

$$2\pi R_m\rho(R_m)+\int_{R<R_m} d\mathbf{R}\frac{\partial\rho}{\partial\mu}\frac{d\mu}{dR_m}=0, \tag{A5}$$

Eq. (A4) is rewritten into

$$2\pi R_m\{G[\rho](R_m)-\mu\rho(R_m)\}$$
$$=2\pi R_m\left\{G[\rho](R_m)-\frac{\delta G[\rho]}{\delta\rho}\rho(R_m)\right\}=0. \tag{A6}$$

In the case of Eq. (5.11) and Eq. (5.12), Eq. (A6) reduces $\rho^2(R_m)=0$ and we have Eqs. (5.16)–(5.18). In the case of Eqs. (5.20), (5.21), and (5.12), we have Eqs. (5.25) and (5.26). [Note that, in the latter case, $\rho(R)$ has a discontinuity at $R=R_m$ and $\lambda^2\rho(R_m)=\lambda^2\rho(R_m-0)=(a/2\pi)^2>0$.]

[1] H. Thomas, G.E. Morfill, V. Demmel, J. Goree, B. Feuerbacher, and D. Möhlmann, Phys. Rev. Lett. **73**, 652 (1994).

[2] J.H. Chu and I. Lin, Physica A **205**, 183 (1994); Phys. Rev. Lett. **72**, 4009 (1994).

[3] Y. Hayashi and K. Tachibana, Jpn. J. Appl. Phys., Part 2 **33**, L804 (1994).

[4] A. Melzer, T. Trottenberg, and A. Piel, Phys. Lett. A **191**, 301 (1994).

[5] H. Totsuji, T. Kishimoto, and C. Totsuji, Phys. Rev. Lett. **78**, 3113 (1997).

[6] H. Totsuji, T. Kishimoto, and C. Totsuji, Jpn. J. Appl. Phys., Part 1 **36**, 4980 (1997).

[7] H. Totsuji, T. Kishimoto, C. Totsuji, and T. Sasabe Phys. Rev. E **58**, 7831 (1998).

[8] W.-T. Juan, Z.-H. Huang, J.-W. Hsu, Y.-J. Lai, and I. Lin, Phys. Rev. E **58**, R6947 (1998).

[9] J. Goree, D. Samsonov, Z. W. Ma, A. Bhattacharjee, H. M. Thomas, U. Konopka, and G. E. Morfill, in *Frontiers in Dusty Plasmas*, Proceedings of the Second International Conference on the Physics of Dusty Plasmas, edited by Y. Nakamura, T. Yokota, and P. K. Shukla (Elsevier, Amsterdam, 2000), p. 91.

[10] V.M. Bedanov and F. Peeters, Phys. Rev. B **49**, 2667 (1994).

[11] V.A. Schweigert and F. Peeters, Phys. Rev. B **51**, 7700 (1995).

[12] I.V. Schweigert, V.A. Schweigert, A. Melzer, and F. Peeters, Phys. Rev. E **62**, 1238 (2000).

[13] A preliminary result has been given in, H. Totsuji, C. Totsuji, K. Tsuruta, K. Kamon, T. Kishimoto, and T. Sasabe, in *Frontiers in Dusty Plasmas* (Ref. [9]), p. 141.

[14] See, for example, F. F. Chen, *Introduction to Plasma Physics* (Plenum, New York, 1974), Chap. 8.

[15] See, for example, S. Pfalzner, and P. Gibbon, *Many-Body Tree Method in Physics* (Cambridge University Press, Cambridge, 1996).

[16] S. Nosé, J. Chem. Phys. **81**, 511 (1984); H.C. Anderson, *ibid.* **72**, 2384 (1980).